Clim. Past Discuss., 4, 1061–1088, 2008
www.clim-past-discuss.net/4/1061/2008/

Climate
of the Past
Discussions

Climate of the Past Discussions is the access reviewed discussion forum of *Climate of the Past*

Strong asymmetry of hemispheric climates during MIS-13 inferred from correlating China loess and Antarctica ice records

Z. T. Guo[1], A. Berger[2], Q. Z. Yin[2], and L. Qin[1,3]

[1]Key Laboratory of Cenozoic Geology and Environment, Institute of Geology and Geophysics, Chinese Academy of Sciences, P.O. Box 9825, Beijing, 100029, China
[2]Institut d'Astronomie et de Géophysique G. Lemaître, Université Catholique de Louvain, Chemin du Cyclotron 2, 1348 Louvain-la-Neuve, Belgium
[3]Graduate School of the Chinese Academy of Sciences, Beijing 100039, China

Received: 27 August 2008 – Accepted: 29 August 2008 – Published: 1 October 2008

Correspondence to: Z. T. Guo (ztguo@mail.iggcas.ac.cn)

Published by Copernicus Publications on behalf of the European Geosciences Union.

Abstract

The loess-soil sequence in northern China is among the best long-term terrestrial climate records in the Northern Hemisphere that documented the history of the Asian summer and winter monsoon circulations, dust emission and aridity of inland deserts. In the Southern Hemisphere, the Antarctica ice cores provided a 800-thousand year (ka) history of the atmospheric methane (CH_4) and carbon dioxide (CO_2) concentrations, eolian dust and Antarctica temperature. We correlate the two records to address the hemispheric climate link in the past 800 ka and the potential roles of Asian dust and monsoon on the atmospheric CO_2 and CH_4 levels. The results show a broad coupling between the Asian and Antarctic climates at the glacial-interglacial scale and support a potential role of Asian dust and monsoon in modulating the atmospheric concentration of greenhouse gases. However, a number of decoupled aspects are revealed, among which marine isotope stage (MIS) 13 exhibits the strongest anomalous link compared with the other interglacials. It is characterized by the greatest interglacial global ice volume, carbon isotope ($\delta^{13}C$) maxima in the world oceans, cooler Antarctic temperature, more extended sea ice in the Southern Ocean, lower CO_2 and CH_4 concentrations, but by unusually strengthened Asian, Indian and African monsoons, weakest Asian winter monsoon, lowest Asian dust and iron fluxes. Particularly warm conditions were also reported for the elevated Tibetan Plateau and northern high-latitude regions. These lines of evidence consistently suggest an increased ice volume in the Southern Hemisphere, a substantially reduced ice volume in the Northern Hemisphere during MIS-13, and hence, an enhanced hemispheric asymmetry of polar ice-conditions. This event has deeply affected the continental, marine and atmospheric conditions at the global scale. Similar anomalies of lesser extents also occurred during MIS-11 and MIS-5e. These suggest that hemispheric climate coupling at the glacial-interglacial scale was significantly unstable during the mid-Pleistocene, and that the degree of asymmetry of polar ice-conditions has prominent impacts on the global climate system, including the Asian monsoon climate. Because global sea ice is likely evolving towards a similar

trend now, the scenario may also be helpful for future climate evaluation.

1 Introduction

Hemispheric glacial-interglacial covariance is a basic feature of the Pleistocene climate system (Ruddiman, 2003; Schmittner et al., 2003). Climate linkages between the two hemispheres have been better examined for the late Quaternary based on ice (Hinnov et al., 2002; Barbante et al., 2006), marine (Pahnke and Zahn, 2005) and some terrestrial records (Lowell et al., 1995). However, much remains to be known about the extent and stability of hemispheric coupling of long-term continental climate changes. Continuous terrestrial records from different geographic locations are particularly valuable for contributing to solve the problem.

The monsoons and inland deserts in Asia are among the key components of the Northern Hemisphere climate system. Their history has been traced back to ~22 million years (Ma) ago (Guo et al., 2002) and is well recorded by the loess deposits in China (An et al., 1990; Ding et al., 1995; Porter and An, 1995; Guo et al., 2000, 2002). Asian monsoon may be the strongest among the global monsoon circulations (Wang, 2006) and would have prominent impacts on the atmospheric CH_4 concentration through modulating the extent of wetlands (Ruddiman, 2003; Loulergue et al., 2008). Deserts in the Asian inlands are an important source of global eolian dust (Kohfeld and Harrison, 2001), which may affect radiation balance of the atmosphere by absorbing or reflecting the incoming solar radiation (Cox et al., 2008), and influence ocean CO_2 uptake capacity by modulating the amount of micronutrients (particularly iron) to the ocean (Ridgwell, 2003; Lambert et al., 2008; Winckler et al., 2008).

The emitted dust from the Asian inlands was transported by the Asian winter monsoon and deposited in the Loess Plateau in northern China (Fig. 1) where annual rainfall is mainly brought by the Asian summer monsoon (An et al., 1990; Ding et al., 1995; Porter and An, 1995; Guo et al., 2004). These led to the formation of the loess-soil alternations with soils corresponding to strengthened summer monsoon and loess to strengthened winter monsoon. Because the summer and winter monsoon circulations originate from northern low- and high-latitudes, respectively, the China loess bears climate information of hemispheric significance.

In the Southern Hemisphere, the Antarctic ice records have recently been extended to ~800 thousand years (ka) ago. The δD record provides a reliable history of Antarctic temperature changes (Jouzel et al., 2007). Analyses on the air bubbles yield a high-resolution history of the atmospheric concentrations of greenhouse gases (Petit et al., 1999; Siegenthaler et al., 2005; Loulergue et al., 2008; Luthi et al., 2008). The eolian dust contained in the ice cores bears valuable information in relation to the atmospheric circulation and the climate conditions of the dust source regions in the Southern Hemisphere (Lambert et al., 2008). Correlating the China loess with the Antarctic ice records provides an ideal opportunity to evaluate the hemispheric climate link over the past 800 ka and the potential impacts of Asian dust and monsoon climate on the atmospheric concentration of greenhouse gases. These are the main aims of this study.

2 Materials and methods

We use the Quaternary loess sections at Xifeng and Changwu in northern China (Fig. 1) to generate the proxies of Asian climates for the last 800 ka. Major interglacial soils and glacial loess units of this portion are labeled S0, L1, S1, L2, S2, ..., S7 and L8 from the top to the bottom with the S5 soil unit subdivided into S5-1, S5-2 and S5-3 (Fig. 2a). Their correlation with the marine δ^{18}O stratigraphy has been commonly accepted (Hovan et al., 1989; Kukla et al., 1990; Ding et al., 1995; Guo et al., 2000). Climate proxies were obtained from samples at 10-cm intervals (723 from Xifeng and 715 from Changwu), representing an average temporal resolution of ~800 years for loess and ~2000 years for soils.

Magnetic susceptibility is widely used as an indicator for soil/loess boundaries (Hovan et al., 1989; Kukla et al., 1990; Ding et al., 1995; Guo et al., 2000). Time controls for the loess timescales are determined through correlating magnetic susceptibility with the marine oxygen isotope ($\delta^{18}O$) record (Lisiecki and Raymo, 2005) (Fig. 2a) and interpolated using a magnetic susceptibility model (Kukla et al., 1990). Although different timescales are available for the Quaternary loess of China (Kukla et al., 1990; Ding et al., 1995; Heslop et al., 2000), there is no major difference between them for the last 800 ka.

Loess accumulation rate (LAR) (Fig. 2b) is a proxy of dust intensity that is mainly determined by the aridity of the source regions in the Asian interior (Hovan et al., 1989; Porter and An, 1995; Guo et al., 2004). The Fe_2O_3 flux in the China loess, which would provide a proportionally quantitative constraint on the eolian iron input from Asia to the ocean, is calculated from the Fe_2O_3 content (Fed) multiplied by sedimentation rate and the mean dust density of 2.5 g cm^{-3}.

Loess grain-size, especially the contents of the coarse fractions (Fig. 2e), primarily reflects the strength of the Asian winter monsoon (Porter and An, 1995; Ding et al., 1995; Guo et al., 2004), as stronger winds transport coarser dust particles. Grain-size of the Xifeng samples was measured using a Malvern Mastersizer-2000 laser analyzer with an analytical precision of about 1%. Samples were pre-treated with hydrogen peroxide to remove organic matter, then with hydrochloric acid to remove carbonates, and with sodium hexametaphosphate for dispersion.

Chemical weathering indexes (Fig. 3a) of the China loess are widely used to document the effects of the summer monsoon because soil formation and chemical weathering in the Loess Plateau primarily depend on the monsoon-related summer moisture and temperature (Guo et al., 1998, 2000; Rousseau and Kukla, 2000; Vidic et al., 2000). Its validity has been confirmed by biological (Rousseau and Kukla, 2000; Rousseau et al., 2000), pedological (Guo et al., 1998, 2000) and rock magnetic studies (Vidic et al., 2000). The ratio between free Fe_2O_3 (Fed), mainly of pedological origin (Singer et al., 1992; Vidic et al., 2000), and total Fe_2O_3 (Fet) is a measurement of the quantity of iron liberated from iron-bearing silicate minerals by chemical weathering relative to the total iron available. The index is widely used by pedologists (Duchaufour, 1983) to assess the chemical weathering of soils and has also been successfully used for documenting the intensity of chemical weathering of the China loess (Guo et al., 1998, 2000). Magnetic susceptibility and Fed/Fet data are from Guo et al. (2000).

The degree of reddening of the soils in loess is indicative of pedogenic intensity and largely reflects soil temperature (Guo et al., 1998, 2000; Yang and Ding, 2003). Redness is measured on samples from Xifeng using a Minolta-CM2002 spectrophotometer with an analytical precision of ∼10% and is expressed as the ratio of red versus total reflectance.

3 Results and discussions

3.1 Broad coupling and decoupled aspects of hemispheric climates in the past 800 ka

Similar to the Antarctic dust flux (Lambert et al., 2008), dust intensity in Asia (Fig. 2b), as is determined by the aridity changes in the Asian inlands, matches overall the glacial-interglacial cycles with higher values for glacial times. However, the relative glacial-interglacial variability is smaller and the average intensity is much higher in Asia than for Antarctica (Fig. 2d). Because the drylands in the Southern Hemisphere are the dominant sources for the Antarctic dust (Revel-Rolland et al., 2006; Lambert et al., 2008), the EDC dust flux would largely reflect the source aridity. Similar glacial-interglacial cycles of dust flux were also observed from the equatorial Pacific (Fig. 2d) (Winckler et al., 2008). These indicate a global-scale link of desert aridity, dust generation and glacial-interglacial changes, attributable to the modulation of the glacial-interglacial variations on the global hydrological cycle.

Particle size of loess and eolian dust in marine sediments primarily reflects the wind strength (Hovan et al., 1989; Ding et al., 1995; Porter and An, 1995; Guo et al., 2004). Dust size in the China loess exhibits variations similar to those of the dust intensity following the glacial-interglacial cycles with coarser dust during glacial times (Fig. 2e). Although the two proxies of the China loess have different implications, their coupled changes at various scales have been firmly demonstrated, and attributed to the Siberian high-pressure cell that influences both Asian aridity and winter monsoon (Porter and An, 1995; Ding et al., 1995; Guo et al., 2004). Dust size in Antarctica may be influenced by several factors (Lambert et al., 2008), but the overall negative correlation with Asian dust size (Fig. 2e) indicates a close coupling of the atmospheric circulation between the two hemispheres.

The consistent changes in the dust intensities in Asia, Antarctica and equatorial Pacific (Fig. 2) suggest a global-scale increase in the atmospheric dust load and in the input of eolian micronutrients to the ocean during glacial times. This is also shown by the iron flux (Fig. 2b) in the China loess that provides a proportionally constraint on the eolian iron input from Asia to the ocean in the past 800 ka. Dust-related micronutrients may affect atmospheric CO_2 level through modulating ocean productivity (Ridgwell, 2003; Lambert et al., 2008; Winckler et al., 2008). Although glacial-interglacial CO_2 changes may relate to a number of factors (Petit et al., 1999; Luthi et al., 2008), the covariance between CO_2 concentration and globally co-varied dust intensities over the past 800 ka supports a close link between them, as well as a partial role in modulating the glacial-interglacial climate contrasts.

The effect on the environment of the Asian summer monsoon in northern China, as reflected by the chemical weathering of loess (Fig. 3a), also exhibits broadly consistent changes along with the glacial-interglacial cycles. Strong summer monsoon matches high peaks of CH_4 concentration. This supports the link between the monsoon climate and atmospheric CH_4 concentration (Ruddiman, 2003; Loulergue et al., 2008) although other wetlands also play an important role (Loulergue et al., 2008).

Chemical weathering of silicate materials (Gaillardet et al., 1999) may affect atmospheric CO_2 concentration by consuming CO_2. However, strong chemical weathering of loess is correlative with high CO_2 level (Figs. 2c and 3a), suggesting that this process within the Asia monsoon zone was not a predominant factor for the glacial-interglacial CO_2 changes.

The correlations therefore show broadly coupled changes of climates between the Asian and Antarctic continents in the past 800 ka and suggest a potentially important role of Asian dust and monsoon in modulating the atmospheric concentrations of greenhouse gases.

However, the correlations also show some obvious decoupled features between the Asian and Antarctic climates. Prominent decoupling includes at least the following aspects.

1. The Antarctic temperature, as reflected by the EDC δD record (Fig. 3b), shows a prominent change at ~430 ka (the Mid-Brunhes Event, MBE), characterized by large increases in the interglacial temperature since then, but slightly decreased glacial temperature (Jouzel et al., 2007). The averagely increased grain-size (winter monsoon) and dust intensity (inland aridity) in Asia during the glacial times after 430 ka is roughly consistent with this transition. However, the transition is not clear in the interglacial records of the Asian summer monsoon (Fig. 3a), winter monsoon (Fig. 2e) and inland aridity (Fig. 2b).
2. Although the MIS-13 temperature in Antarctica was lower than for most of the other interglacials of the past 800 ka, the strongest summer monsoon, weakest winter monsoon and lowest inland aridity in Asia was recorded in the China loess for this time, and to a lesser extent, for MIS-11 and 5e (Fig. 3a).
3. The largely weakened Asian summer monsoon during the glacial times (Fig. 3a) matches the low glacial temperature in Antarctica (Fig. 3b). However, a number of intervals with relatively weak winter monsoon and low inland aridity within some glacial periods are documented in the China loess, such as in MIS-16, MIS 14, MIS-12 and MIS-3, which have no clear expression in the Antarctic δD record (Fig. 3b). These suggest a greater similarity of the summer monsoon changes to the Antarctic climate during glacial times than for the winter monsoon and inland aridity in Asia.
4. Despite of the general coherencies between high/low Asian dust intensity and low/high CO_2 levels, between strong/weak Asian summer monsoon and high/low

CH_4 levels as discussed above, the fluctuation patterns for both the CO_2 and CH_4 concentrations are, in overall, in better agreements with the Antarctic temperature changes (Siegenthaler et al., 2005; Loulergue et al., 2008) than with the Asian climates in the Northern Hemisphere.

3.2 Anomalous continental, marine and atmospheric conditions during MIS-13

Among these decoupled aspects between the Asian and Antarctic climates, a particularly strong anomaly in the hemispheric climate link is observed for MIS-13 especially when it is compared with the other interglacials of the past 800 ka. This is the main focus of this study.

The EDC δD record indicates a much cooler MIS-13 interglacial in Antarctica (Fig. 3b) with a temperature ∼4°C lower than for the Holocene (Jouzel et al., 2007). EDC dust flux (Lambert et al., 2008) is averagely higher during MIS-13 than during the younger interglacials, indicating a greater aridity in the dust source regions of the Southern Hemisphere. Marine $\delta^{18}O$ record (Lisiecki and Raymo, 2005) indicates the largest global ice volume among the interglacials of the past 800 ka (Fig. 2a).

However, the China loess records the lowest inland aridity (Fig. 2b), an extremely weak winter monsoon (Fig. 2e) and an extremely strong summer monsoon (Fig. 3a). MIS-13 corresponds to the strongest soil (S5-1) among all the Quaternary soils in the China loess (Fig. 2a). Over the Loess Plateau, we estimate that the mean annual temperature increased by at least 4–6°C and the annual rainfall by 200–300 mm compared to today (Guo et al., 1998). Unusually strong Asian summer monsoon is expressed in southern China by the development of the widely spread vermiculated soil complex (Yin and Guo, 2006) that is indicative of extremely warm and humid conditions. Warmer and more humid Asian inlands are also reflected by reduced mass accumulation rates of Asian dust in the North Pacific (Hovan et al., 1989).

The extreme conditions of MIS-13 were not limited within the Asian monsoon zone and inland deserts. MIS-13 was also recognized as the warmest interglacial of the past 800 ka in the elevated Tibetan Plateau from the presence of forest conditions (Chen et al., 1999). Particularly warm conditions were also identified in the non-monsoonal Baikal region (Prokopenko et al., 2002), in northern Europe (Vandenberghe, 2000; Zagwijn, 1996) and Greenland (De Vernal and Hillaire-Marcel, 2008), all located in the high-latitude continents of the Northern Hemisphere. Unusually strong African (Rossignol-Strick et al., 1998) and Indian (Bassinot et al., 1994) monsoons at this time were also recorded respectively by a thick Mediterranean sapropel resulting from high flooding of the Nile river, and by an extreme of low surface salinity in the equatorial Indian Ocean, suggesting commonly strengthened monsoon circulations in the Northern Hemisphere.

In the global ocean, δ^{13}C records of the past 800 ka from the North Atlantic (Raymo et al., 1997; McManus et al., 1999), tropical Atlantic (Raymo et al., 1997), and the Pacific (Raymo et al., 1997) show a global-scale positive anomaly during MIS-13 (Fig. 3c). Atlantic δ^{13}C gradient (Raymo et al., 1997) suggests a strong input of North Atlantic Deep Water (NADW) to the tropical Atlantic. High δ^{13}C values were also clearly present in the Southern Ocean (Oppo et al., 1990) (Fig. 3c). These indicate that the event had links with the ocean circulation and the carbon cycle. ODP 908 site from the North Atlantic shows a total lack of ice-rafted debris (McManus et al., 1999) during a long interval within MIS-13, an only case in the 500-ka record. Although the amount of ice-rafted debris is site-dependent, most of the records from circum-Arctic oceans indicate a much reduced intensity of ice-rafting, typical of a warm interglacial. In contrast, summer sea surface temperature (SSST) in the sub-Antarctic Atlantic was the lowest among the interglacials of the past 550 ka (Becquey and Gersonde, 2003) with widely extended sea ice (Wolff et al., 2006).

Atmospheric conditions were also anomalous during MIS-13. Although dust size (Fig. 2e) in Antarctica has more complicate implications (Lambert et al., 2008), it in any way reflects also the atmospheric conditions. The coarsest EDC dust size during MIS-13, associated with the monsoon changes in the Northern Hemisphere, indicates a prominent change in the atmospheric circulation at the global scale. Reduced dust and iron fluxes (Fig. 2b) during MIS-13 would favour a higher CO_2 concentration because it may reduce marine productivity (Ridgwell, 2003; Lambert et al., 2008; Winckler et al., 2008). However, the atmospheric CO_2 concentration during MIS-13 is the second lowest interglacial value in the past 800 ka after MIS-17 (Fig. 2c).

Monsoonal wetlands in the Northern Hemisphere are among the dominant sources (Ruddiman, 2003; Loulergue et al., 2008) of atmospheric CH_4. The unusually strong Asian, African and Indian monsoons, as well as the warm-humid conditions over the Northern Hemisphere continents during MIS-13 would have led to increased CH_4 emission. However, the atmospheric CH_4 concentration at this time was the lowest among the interglacials of the past 800 ka (Fig. 3b). This anomalous link needs therefore to invoke an offset by a strongly reduced CH_4 emission from the Southern Hemisphere. Thus, the climates in the Southern Hemisphere during MIS-13 must have been generally drier and cooler than for the other interglacials, as is confirmed by the cooler temperature (Jouzel et al., 2007) that generally weakens the hydrological cycle, the averagely higher dust flux at EDC (Lambert et al., 2008), and the more extended sea ice in the Southern Ocean (Wolff et al., 2006). This implies an important role of the Southern Hemisphere lands in modulating the global CH_4 levels beside the prominent roles of the Northern hemisphere lands. This is also consistent with the recent study that a present-day decreasing aerosol pollution in the Northern Hemisphere, as is similar to the case for MIS-13, may cause greater aridity in Amazonian region (Cox et al., 2008), one of the main global CH_4 sources.

Our correlation thus indicates for MIS-13

1. global anomalies in the continental, marine and atmospheric environments;
2. anomalous links of dust, monsoon and greenhouse gases in comparison with the other interglacials; and
3. a strong hemispheric asymmetry of climates marked by averagely cooler and drier conditions in the Southern Hemisphere and generally warmer conditions in the Northern Hemisphere.

3.3 Strong asymmetry of polar ice conditions during MIS-13

We do not attempt to explore the global significance and possible causes of all the decoupled aspects between the China loess and Antarctica ice records. However, the most prominent case, as represented by the MIS-13 anomaly, may be expected to provide helpful insights. Because of the strong imprints of this anomaly in the global continental, marine and atmospheric environments, it would require invoking factors of the global scale.

Summer insolation changes at the northern low-latitudes have deep impacts on the Asian, Indian and African monsoons with insolation maxima resulting in strengthened monsoons (Bassinot et al., 1994; Kutzbach and Liu, 1997; Ruddiman, 2003). Although insolation maxima also occurred within MIS-13 corresponding to MIS-13.3, 13.13 and 13.11 (Berger, 1978), the values are far from being higher than for the other interglacials (Fig. 3d), and consequently, can not alone explain the extremely strengthened monsoons in the Northern Hemisphere.

Because the Asian winter monsoon has a high-latitude origin, its strength is largely dependent of the northern high-latitude conditions. Climate models (Ruddiman and Kutzbach, 1989; Wu and Wang, 2002) and geological records (Ding et al., 1995; Porter and An, 1995; Guo et al., 2004) consistently suggest the strong impacts of the northern ice-sheets and sea-ice on the inland aridity and strength of the winter monsoon in Asia through modulating the winter intensity of the Siberian High. Long-term changes in eolian grain-size and dust intensity of the China loess were closely coupled with the ice-rafting intensity in the circum-Arctic ocean and with the development of the Northern Hemisphere ice-sheets over the past 6 Ma (Guo et al., 2004). The general correlation of the China loess stratigraphy with the marine δ^{18}O record (Fig. 2a) validates this link at the glacial-interglacial scale (Hovan et al., 1989; Kukla et al., 1990; Ding et al., 1995). Ice-rafting events in the North Atlantic led to pulses of strong Asian winter monsoon at millennial scales (Porter and An, 1995). These consistently indicate a close dynamical link of the Asian winter monsoon and inland aridity with the northern ice-sheet/sea ice conditions. Consequently, the lowest source aridity and weakest winter monsoon during MIS-13 in Asia indicate that such an ice forcing was largely weakened.

Marine δ^{18}O record of benthic foraminifera in the past 800 ka is primarily indicative of global ice volume (Ruddiman, 2003; Lisiecki and Raymo, 2005), but does not discriminate signals between the southern and the northern ice-sheets. The above lines of evidence from the regions, where climates have close links with the ice-conditions at northern high-latitudes, strongly contrast an interpretation of the relatively high interglacial δ^{18}O value during MIS-13 as a result of greater ice-sheets in the Northern Hemisphere. Rather, they indicate smaller northern ice-sheets than for the other interglacials, as is consistent with the particularly abundant pollens at this time at ODP site 646 reflecting a substantially reduced Greenland ice sheet (De Vernal and Hillaire-Marcel, 2008). Consequently, the higher interglacial marine δ^{18}O value (Lisiecki and Raymo, 2005) during MIS-13 must reflect a greater ice volume in the Southern Hemisphere although a potential effect of deep ocean temperature on the δ^{18}O signals could not be totally excluded in view of the anomalous ocean conditions. These define MIS-13 as an unusual interglacial, characterized by greater ice volume in Antarctica and smaller one at northern high latitudes, and hence, a much-enhanced asymmetry of ice conditions between the two hemispheres.

This scenario could also explain most of the observed features in the continental, marine and atmospheric environments during MIS-13 according to the following mechanisms yielded by geological records and climate models for some other periods.

Warmer conditions in the Northern Hemisphere continents, particularly in Tibetan Plateau (Chen et al., 1999), largely enhance land-sea thermal contrasts and reinforce summer monsoon circulations (Ruddiman, 2003; Ruddiman and Kutzbach, 1989). This, associated with the precession-driven insolation maxima at northern low-latitudes (Berger, 1978), can partly explain the unusually strengthened monsoons during MIS-13.

Meridional shift of the atmospheric circulation may also be worthy being considered. Today, the inter-tropical convergence zone (ITCZ) penetrates into the Northern Hemisphere in summer as far as to 24° N due to hemispheric asymmetry and reinforces the northern monsoon circulations (Wang, 2005). Climate records and model experiments showed that further shift can be induced by greater extents of sea ice over the Southern Atlantic and Southern Ocean (Iriondo, 2000; Markgraf et al., 2000; Lambert et al., 2008), by cooler temperature in the Southern Hemisphere and by reduced dust aerosol in the Northern Hemisphere (Cox et al., 2008). Because MIS-13 is rightly marked by similar conditions, they would provide a complementary explanation of the strong summer monsoons in the Northern Hemisphere during MIS-13.

A cooler and drier MIS-13 in the Southern Hemisphere would favour a reduced terrestrial biomass, but an overall warmer and more humid Northern Hemisphere would have led to globally increased terrestrial biomass (Duplessy et al., 1984, 2007) and stronger chemical weathering due to its larger land area. This may partly explain the higher marine δ^{13}C values and lower atmospheric CO_2 level. The lower Antarctica temperature and greater global ice volume during MIS-13 also favour a lower CO_2 concentration (Ruddiman, 2003; Siegenthaler et al., 2005; Luthi et al., 2008).

Smaller northern ice-sheets would have also occurred within MIS-11 and MIS-5e, as suggested by the stronger summer monsoon (Fig. 3a), low dust intensity and weak winter monsoon in Asia (Fig. 2b and e). These are consistent with the more abundant pollens during these two periods at ODP site 646 that indicates a reduced Greenland ice-sheet (De Vernal and Hillaire-Marcel, 2008). Marine records also showed δ^{13}C positive anomaly (Oppo et al., 1990; Raymo et al., 1997) (Fig. 3c), greater NADW input to the Southern Ocean (Oppo et al., 1990) and a near-absence of ice-rafting near the Arctic (McManus et al., 1999). However, they differ from MIS-13 by smaller global ice volumes (Fig. 2a), warmer Antarctic temperature (Fig. 3b), and higher CO_2 and CH_4 levels (Figs. 2c and 3b). These suggest smaller southern ice-sheets than for MIS-13, and hence hemispheric asymmetries of a lesser extent.

The cause of the enhanced hemispheric asymmetry of ice conditions during MIS-13 remains to be further addressed. Greenhouse warming may cause similar asymmetry of sea ice (Manabe et al., 1992; Cavalieri et al., 1997), but cannot account for MIS-13 because of its lower CO_2 and CH_4levels.

Insolation should be one of the possible causes. Although the CO_2 concentration was ∼40 ppmv lower (Luthi et al., 2008) in MIS-13 than the pre-industial level (equivalent to a radiative forcing of $\sim -0.82\,\mathrm{Wm^{-2}}$), high northern latitudes received more energy during their summer when this season occurred at perihelion, i.e. three times in MIS-13 at 529, 506, and 485 ka BP. For example, summer insolation at 65° N was $50\,\mathrm{Wm^{-2}}$ higher at 506 ka ago (Fig. 2f) when eccentricity was much larger (Berger, 1978). The consequent net increase of energy received by the northern high-latitudes would favour ice melting. On the contrary, summer insolation at 65° S was $50\,\mathrm{Wm^{-2}}$ lower (Berger, 1978) at 506 ka ago. This, associated with the lower concentrations of greenhouse gases (Loulergue et al., 2008; Luthi et al., 2008), would favour ice building in the Southern Hemisphere. This also happened at 485 ka BP, but at 529 ka BP the amplitude of the seasonal changes anomaly was reduced due to a lower eccentricity. On the other hand, insolation anomalies at MIS-5e were even larger than at 606 ka BP due to a larger eccentricity (Berger, 1978), as is consistent with the stronger summer monsoon (Fig. 3a), weaker winter monsoon and lower dust intensity in Asia (Figs. 2e and 3a). In addition, MIS-13 and MIS-11 coincide with a mid-Pleistocene interval of lower amplitude changes of summer insolation at northern high-latitudes (Berger, 1978) from ∼570 to 340 Kyr (Fig. 2f). The higher values of the insolation minima would disfavour ice building in the Northern Hemisphere.

However, insolation is unlikely to be the only cause because insolation patterns similar to the MIS-13 anomaly also occurred for the times when the monsoons were not necessarily strong (for example MIS-7, 242 ka BP). The initial effects of insolation must have been amplified by internal climate processes. A stronger NADW formation, as suggested by oceanographic data (Raymo et al., 1997; McManus et al., 1999), is among the factors to be considered as it may modulate meridional heat transport (Broecker, 1998), and hence favors climate asymmetry between the two hemispheres. Because NADW has initially heavier $\delta^{13}C$ values and migrates to other marine basins (Duplessy et al., 1984, 2007; Raymo et al., 1997), it also partly explains the $\delta^{13}C$

anomaly in the global ocean. We believe that the largely reinforced northern summer monsoon circulations would have also helped the energy transport to the Northern Hemisphere.

Although hemispheric coupling of the glacial-interglacial changes is a basic feature of the Pleistocene climate system (Ruddiman, 2003; Schmittner et al., 2003), our correlation suggests that ice-conditions in both hemispheres have evolved with relative independence, leading to an unstable coupling of hemispheric climates during the Mid-Pleistocene. The consequent asymmetric ice conditions had strong impacts on the continental, marine and atmospheric conditions at the global scale. The correlation also suggests that marine δ^{18}O values were sometimes more dominated by the signals from one hemisphere, and are not in entire consistency with the ice conditions in the other hemisphere.

This scenario may also have implications for the other decoupled aspects between the China loess and Antarctica ice records of the past 800 ka, and for the evolution of the climate system during other periods of the Quaternary. Because either geological records (Ding et al., 1995; Porter and An, 1995; Guo et al., 2004) or climate models (Ruddiman and Kutzbach, 1989; Wu and Wang, 2002) indicate a close link between the Asian winter monsoon and ice conditions in the northern high-latitudes, we suggest that grain-size of the Quaternary loess in China may be taken as a first attempt at an indication of the average ice conditions in the Northern Hemisphere. The rather ambiguous expression of the MBE transition in the interglacial Asian climate and the weakened winter monsoon/inland aridity within some glacial intervals might also be linked to a weakened ice forcing in the northern high-latitudes. In contrast, the coarsest loess unit L9 (correlative to MIS-22) in China, an indication of particularly strengthened winter monsoon circulation and inland aridity in Asia (Guo et al., 1998), might be linked to substantially increased northern ice-sheets versus smaller ones in the Southern Hemisphere because the globally total ice volume, as indicated by the marine δ^{18}O record (Lisiecki and Raymo, 2005), was not greater than for the other glacial periods. Further understanding of these issues would require new terrestrial and marine records, particularly from the polar regions, to independently trace the evolutions of their ice and climate conditions. Ice modelling would also be of high importance.

Large amplitude waxing and waning of ice-sheets are a relatively slow process at geological scale, but extents of sea ice can vary at century and decadal scales and currently show a decreasing trend in the Northern Hemisphere (Cavalieri et al., 1997). These suggest that the asymmetric scenario similar to that of MIS-13 may operate at shorter-terms and affect future climate. Thus, MIS-13 provides an amplified case and is also helpful for testing and validating climate models.

4 Conclusions

Our correlation between the China loess and the Antarctic ice records showed the following main insights related to the hemispheric climate link over the past 800 ka.

1. The climates in Asia and Antarctica were broadly coupled at the glacial-interglacial scale over the past 800 ka, as is consistent with the other Pleistocene climate records from both hemispheres. General coherencies are observed between high/low Asian dust intensity and low/high CO_2 levels, between strong/weak Asian summer monsoon and high/low CH_4 concentrations following the glacial-interglacial cycles. These support the potential impacts of the Asian dust and monsoon in modulating the atmospheric concentration of CO_2 and CH_4, and hence, a partial role in amplifying the glacial-interglacial cycles. The iron flux from the China loess provides a proportionally quantitative constraint on the eolian iron input from Asia to the ocean. The clear negative correlation of dust size between the China loess and the Antarctica ice records indicate a close hemispheric coupling of the atmospheric circulation.

2. The correlation reveals a number of decoupled aspects between the two records. Among them, a particularly strong anomalous link of hemispheric climates is observed for MIS-13 compared with the other interglacials. It was characterized by

greater global ice volume, ocean carbon isotope (δ^{13}C) maxima, cooler Antarctic temperature, lower CO_2 and CH_4 concentrations, but by extremely strong Asian, Indian and African summer monsoons in the Northern Hemisphere, weakest Asian winter monsoon, lowest Asian dust and iron fluxes, extremely warm conditions on the elevated Tibetan Plateau and in the northern high-latitude regions. Comprehensive examinations on the relevant geological records consistently suggest a greater ice volume in the Southern Hemisphere, a significantly reduced ice volume in the Northern Hemisphere, and hence, an enhanced hemispheric asymmetry of polar ice conditions during MIS-13. Our loess records and the pollen record near Greenland (De Vernal and Hillaire-Marcel, 2008) suggest that smaller northern ice-sheets would have also occurred during MIS-11 and MIS-5e, with apparently a lesser extent of hemispheric asymmetry than for MIS-13.

3. The cause of the strong asymmetry of hemispheric climates during MIS-13 remains to be further addressed. An initial effect of insolation amplified by the ocean and atmospheric circulations are likely factors to be considered. Climate model experiments would be of particular values. However, the present study suggests that the climates of the two hemispheres could be significantly decoupled under specific conditions, and that the consequent asymmetric ice conditions may cause global anomalies in the continental, marine and atmospheric conditions, including the Asian monsoon circulations. These may also have implications for the other decoupled aspects and for other periods of the Quaternary. MIS-13 also provides an amplified case for future climate evaluation because the current extents of sea ice are likely evolving towards a similar asymmetrical trend.

Acknowledgements. This research was supported by grants from Chinese Academy of Sciences (KZCX2-YW-117) and National Natural Science Foundation of China (40730104). Q. Yin benefits from a postgraduate grant from Université Catholique de Louvain. Z. T. Guo thanks D. Raynaud for the valuable suggestions and discussions.

References

An, Z. S., Liu, T. S., Lu, Y. C., Porter, S. C., Kukla, G., Wu, X. H., and Hua, Y. M.: The long-term paleomonsoon variation recorded by the loess-paleosol sequence in Central China, Quat. Int., 7–8, 91–95, 1990.

Barbante, C., Barnola, J.-M., Becagli, S., et al.: One-to-one coupling of glacial climate variability in Greenland and Antarctica, Nature, 444, 195–198, 2006.

Bassinot, F. C., Labeyrie, L. D., Vincent, E., Quidelleur, X., Shackleton, N. J., and Lancelot, Y.: The astronomical theory of climate and the age of the Brunhes-Matuyama magnetic reversal, Earth Planet. Sci. Lett., 126, 91–108, 1994.

Becquey, S. and Gersonde, R.: A 0.55-Ma paleotemperature record from the Subantarctic zone: Implications for Antarctic Circumpolar Current development, Paleoceanography, 18, 1014, doi:10.1029/2000PA000576, 2003.

Berger, A.: Long-term variations of daily insolation and Quaternary climate changes, J. Atmos. Sci., 35, 2362–2367, 1978.

Broecker, W. S.: Paleocean circulation during the last deglaciation: a bipolar seesaw?, Paleoceanography, 13, 119–121, 1998.

Cavalieri, D. J., Gloersen, P., Parkinson, C. L., Comiso, J. C., and Zwally, H. J.: Observed hemispheric asymmetry in global sea ice changes, Science, 278, 1104–1106, 1997.

Chen, F. H., Bloemendal, J., Zhang, P. Z., and Liu, G. X.: An 800 ky proxy record of climate from lake sediments of the Zoige Basin, eastern Tibetan Plateau, Palaeogeogr. Palaeocl., 151, 307–320, 1999.

Cox, P. M., Harris, P. P., Huntingford, C., Betts, R. A., Collins, M., Jones, C. D., Jupp, T. E., Marengo, J. A., and Nobre, C. A.: Increasing risk of Amazonian drought due to decreasing aerosol pollution, Nature, 453, 212–215, 2008.

De Vernal, A. and Hillaire-Marcel, C.: Natural variability of Greenland climate, vegetation, and ice volume during the past million years, Science, 320, 1622–1625, 2008.

Ding, Z. L., Liu, T. S., Rutter, N. W., Yu, Z. W., Guo, Z. T., and Zhu, R. X.: Ice-volume forcing of East Asian winter monsoon variations in the past 800 000 years, Quat. Res., 44, 149–159, 1995.

Duchaufour, P.: Pedologie, Tome 1: pedogenese et Classification, Masson, Paris, France, New York, USA, Barcelone, Spain, and Milan, Italy, 1983.

Duplessy, J. C., Shackleton, N. J., Matthews, R. K., Prell, W., Ruddiman, W. F., Caralp, M., and

Hendy, C. H.: ^{13}C record of benthic foraminifera in the last interglacial ocean: implications for the carbon cycle and the global deep water circulation, Quat. Res., 21, 225–243, 1984.

Duplessy, J. C., Roche, D. M., and Kageyama, M.: The deep ocean during the last interglacial period, Science, 316, 89–91, 2007.

Gaillardet, J., Dupre, B., Louvat, P., and Allegre, C. J.: Global silicate weathering and CO_2 consumption rates deduced from the chemistry of large rivers, Chemical Geol., 159, 3–30, 1999.

Guo, Z. T., Biscaye, P., Wei, L. Y., Chen, X. H., Peng, S. Z., and Liu, T. S.: Summer monsoon variations over the last 1.2 Ma from the weathering of loess-soil sequences in China, Geophys. Res. Lett., 27, 1751–1754, 2000.

Guo, Z.T., Peng, S.Z., Hao, Q.Z., Biscaye, P. E., An, Z. S., and Liu, T. S.: Late Miocene-Pliocene development of Asian aridification as recorded in the Red-Earth Formation in northern China, Global Planet. Change, 41, 135–145, 2004.

Guo, Z. T., Liu, T. S., Fédoroff, N., Wei, L. Y., Ding, Z. L., Wu, N. Q., Lu, H. Y., Jiang, W. Y., and An, Z. S.: Climate extremes in loess of China coupled with the strength of deep-water formation in the North Atlantic, Global Planet. Change, 18, 113–128, 1998.

Guo, Z. T., Ruddiman, W. F., Hao, Q. Z., Wu, H. B., Qiao, Y. S., Zhu, R. X., Peng, S. Z., Wei, J. J., Yuan, B. Y., and Liu, T. S.: Onset of Asian desertification by 22 Myr ago inferred from loess deposits in China, Nature, 416, 159–163, 2002.

Heslop, D., Langereis, C. G., and Dekkers, M. J.: A new astronomical timescale for the loess deposits of Northern China, Earth Planet. Sci. Lett., 184, 125–139, 2000.

Hinnov, L. A., Schulz, M., and Yiou, P.: Interhemispheric space-time attributes of the Dansgaard-Oeschger oscillations between 100 and 0 ka, Quat. Sci. Rev., 21, 1213–1228, 2002.

Hovan, S. A., Rea, D. K., Pisias, N. G., and Shackleton, N. J.: A direct link between the China loess and marine ^{18}O records: aeolian flux to the north Pacific, Nature, 340, 296–298, 1989.

Iriondo, M.: Patagonian dust in Antarctica, Quat. Int., 68, 83–86, 2000.

Jouzel, J., Masson-Delmotte, V., Cattani, O., Dreyfus, G., Falourd, S., Hoffmann, G., Minster, B., Nouet, J., Barnola, J. M., Chappellaz, J., Fischer, H., Gallet, J. C., Johnsen, S., Leuenberger, M., Loulergue, L., Luethi, D., Oerter, H., Parrenin, F., Raisbeck, G., Raynaud, D., Schilt, A., Schwander, J., Selmo, E., Souchez, R., Spahni, R., Stauffer, B., Steffensen, J. P., Stenni, B., Stocker, T. F., Tison, J. L., Werner, M., and Wolff, E. W.: Orbital and millennial Antarctic climate variability over the past 800 000 years, Science, 317, 793–796, 2007.

Kohfeld, K. E. and Harrison, S. P.: DIRTMAP: the geological record of dust, Earth-Sci. Rev., 54, 81–114, 2001.

Kukla, G., An, Z. S., Melice, J. L., Gavin, J., and Xiao, J. L.: Magnetic susceptibility record of Chinese Loess, T. Roy. Soc. Edin.-Earth, 81, 263–288, 1990.

Kutzbach, J. E. and Liu, Z.: Response of the African monsoon to orbital forcing and ocean feedbacks in the middle Holocene, Science, 278, 440–443, 1997.

Lambert, F., Delmonte, B., Petit, J. R., Bigler, M., Kaufmann, P. R., Hutterli, M. A., Stocker, T. F., Ruth, U., Steffensen, J. P., and Maggi, V.: Dust-climate couplings over the past 800 000 years from the EPICA Dome C ice core, Nature, 452, 616–619, 2008.

Lisiecki, L. E. and Raymo, M. E.: A Pliocene-Pleistocene stack of 57 globally distributed benthic δ^{18}O records, Paleoceanography, 20, PA1003, doi:10.1029/2004PA001071, 2005.

Loulergue, L., Schilt, A., Spahni, R., Masson-Delmotte, V., Blunier, T., Lemieux, B., Barnola, J. M., Raynaud, D., Stocker, T. F., and Chappellaz, J.: Orbital and millennial-scale features of atmospheric CH_4 over the past 800 000 years, Nature, 453, 383–386, 2008.

Lowell, T. V., Heusser, C. J., Andersen, B. G., Moreno, P. I., Hauser, A., Heusser, L. E., Schluchter, C., Marchant, D. R., and Denton, G. H.: Interhemispheric correlation of Late Pleistocene glacial events, Science, 269, 1541–1549, 1995.

Luthi, D., Le Floch, M., Bereiter, B., Blunier, T., Barnola, J. M., Siegenthaler, U., Raynaud, D., Jouzel, J., Fischer, H., Kawamura, K., and Stocker, T. F.: High-resolution carbon dioxide concentration record 650 000–800 000 years before present, Nature, 453, 379–382, 2008.

Markgraf, V., Baumgartner, T. R., Bradbury, J. P., Diaz, H. F., Dunbar, R. B., Luckman, B. H., Seltzer, G. O., Swetnam, T. W., and Villalba, R.: Paleoclimate reconstruction along the Pole-Equator-Pole transect of the Americas (PEP 1), Quat. Sci. Rev., 19, 125–140, 2000.

Manabe, S., Spelman, M. J., and Stouffer, R. J.: Transient responses of a coupled ocean atmosphere model to gradual changes of atmospheric CO_2. 2. Seasonal response, J. Climate, 5, 105–126, 1992.

McManus, J. F., Oppo, D. W., and Cullen, J. L.: A 0.5-million-year record of millennial-scale climate variability in the North Atlantic, Science, 283, 971–975, 1999.

Oppo, D. W., Fairbanks, R. G., and Gordon, A. L.: Late Pleistocene Southern Ocean δ^{13}C variability, Paleoceanography, 5, 43–54, 1990.

Pahnke, K. and Zahn, R.: Southern hemisphere water mass conversion linked with North Atlantic climate variability, Science, 307, 1741–1746, 2005.

Parrenin, F., Barnola, J. M., Beer, J., Blunier, T., Castellano, E., Chappellaz, J., Dreyfus, G., Fischer, H., Fujita, S., Jouzel, J., Kawamura, K., Lemieux-Dudon, B., Loulergue, L., Masson-Delmotte, V., Narcisi, B., Petit, J. R., Raisbeck, G., Raynaud, D., Ruth, U., Schwander, J., Severi, M., Spahni, R., Steffensen, J. P., Svensson, A., Udisti, R., Waelbroeck, C., and Wolff, E.: The EDC3 chronology for the EPICA Dome C ice core, Clim. Past, 3, 485–497, 2007, http://www.clim-past.net/3/485/2007/.

Petit, J. R., Jouzel, J., Raynaud, D., Barkov, N. I., Barnola, J.-M., Basile, I., Bender, M., Chappellaz, J., Davisk, M., Delaygue, G., Delmotte, M., Kotlyakov, V. M., Legrand, M., Lipenkov, V. Y., Lorius, C., Pepin, L., Ritz, C., Saltzmank, E., and Stievenard, M.: Climate and atmospheric history of the past 420 000 years from the Vostok ice core, Antarctica, Nature, 399, 429–436, 1999.

Porter, S. C. and An, Z. S.: Correlation between climate events in the North Atlantic and China during the last glacial maximum, Nature, 375, 305–308, 1995.

Prokopenko, A. A., Williams, D. F., Kuzmin, M. I., Karabanov, E. B., Khursevich, G. K., and Peck, J. A.: Muted climate variations in continental Siberia during the mid-Pleistocene epoch, Nature, 418, 65–68, 2002.

Raymo, M. E., Oppo, D. W., and Curry, W.: The mid-Pleistocene climate transition: A deep sea carbon isotopic perspective, Paleoceanography, 12, 546–559, 1997.

Revel-Rolland, M., De Deckker, P., Delmonte, B., Hesse, P. P., Magee, J. W., Basile-Doelsch, I., Grousset, F., and Bosch, D.: Eastern Australia: A possible source of dust in East Antarctica interglacial ice, Earth Planet. Sci. Lett., 249, 1–13, 2006.

Ridgwell, A. J.: Implications of the glacial CO_2 “iron hypothesis” for Quaternary climate change, Geochem. Geophy. Geosy., 4, 1076, doi:1010.1029/2003GC000563, 2003.

Rossignol-Strick, M., Paterne, M., Bassinot, F. C., Emeis, K. C., and De Lange, G. J.: An unusual mid-Pleistocene monsoon period over Africa and Asia, Nature, 392, 269–272, 1998.

Rousseau, D.-D., Wu, N. Q., and Guo, Z. T.: The terrestrial molluscs as new indices of the Asian paleomonsoons in the Chinese loess plateau, Global Planet. Change, 26, 199–206, 2000.

Rousseau, D.-D. and Kukla, G.: Abrupt retreat of summer monsoon at the S1/L1 boundary in China, Global Planet. Change, 26, 189–198, 2000.

Ruddiman, W. F. and Kutzbach, J. E.: Forcing of late Cenozoic northern hemisphere climate by plateau uplift in southern Asia and the American West, J. Geophys. Res., 94, 18 409–18 427, 1989.

Ruddiman, W. F.: Orbital insolation, ice volume, and greenhouse gases, Quat. Sci. Rev., 22, 1597–1629, 2003.

Schmittner, A., Saenko, O. A., and Weaver, A. J.: Coupling of the hemispheres in observations and simulations of glacial climate change, Quat. Sci. Rev., 22, 659–671, 2003.

Siegenthaler, U., Stocker, T. F., Monnin, E., Luthi, D., Schwander, J., Stauffer, B., Raynaud, D., Barnola, J. M., Fischer, H., Masson-Delmotte, V., and Jouzel, J.: Stable carbon cycle-climate relationship during the late Pleistocene, Science, 310, 1313–1317, 2005.

Singer, M. J., Fine, P., Verosub, K. L., and Chadwick, O. A.: Time dependence of magnetic susceptibility of soil chronosequences on the California coast, Quat. Res., 37, 323–332, 1992.

Vandenberghe, J.: A global perspective of the European chronostratigraphy for the past 650 ka, Quat. Sci. Rev., 19, 1701–1707, 2000.

Vidic, N. J., TenPas, J. D., Verosub, K. L., and Singer, M. J.: Separation of pedogenic and lithogenic components of magnetic susceptibility in the Chinese loess/palaeosol sequence as determined by the CBD procedure and a mixing analysis, Geophys. J. Int., 142, 551–562, 2000.

Wang, B.: The Asian Monsoon, Springer-Verlag, Berlin-Heidelberg-New York, 844 pp., 2006.

Winckler, G., Anderson, R. F., Fleisher, M. Q., McGee, D., and Mahowald, N.: Covariant glacial-interglacial dust fluxes in the equatorial Pacific and Antarctica, Science, 320, 93–96, 2008.

Wolff, E. W., Fischer, H., Fundel, F., et al.: Southern Ocean sea-ice extent, productivity and iron flux over the past eight glacial cycles, Nature, 440, 491–496, 2006.

Wu, B. Y. and Wang, J.: Possible impacts of winter Arctic Oscillation on Siberian high, the East Asian winter monsoon and sea-ice extent, Adv. Atmos. Sci., 19, 297–320, doi:10.1007/S003760020024, 2002.

Yang, S. L. and Ding, Z. L.: Color reflectance of Chinese loess and its implications for climate gradient changes during the last two glacial-interglacial cycles, Geophys. Res. Lett., 30, 2058, doi:2010.1029/2003GL018346, 2003.

Yin, Q. Z. and Guo, Z. T.: Mid-Pleistocene vermiculated red soils in southern China as an indication of unusually strengthened East Asian monsoon, Chinese Sci. Bull., 51, 213–220, 2006.

Zagwijn, W.: The cromerian complex stage of the Netherlands and correlation with other areas in Europe, in: The early Middle Pleistocene in Europe, edited by: Tunrner, C., Balkema, Rotterdam, The Netherlands, 145–172, 1996.

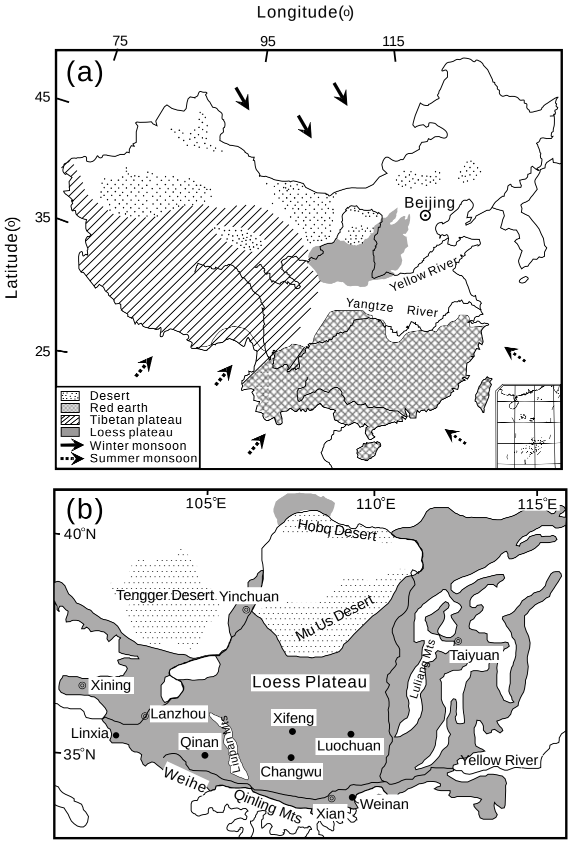

Fig. 1. Maps showing the modern environmental pattern and Loess Plateau in China. **(a)** Modern environmental pattern and the prevailing atmospheric circulation. Dotted arrows indicate the southwest and southeast Asian summer monsoons and solid arrows indicate the Asian winter monsoon. **(b)** Loess Plateau in China and the studied sites.

Title Page
Abstract
Introduction
Conclusions
References
Tables
Figures
◀◀
▶▶
◀
▶
Back
Close
Full Screen / Esc
Printer-friendly Version
Interactive Discussion

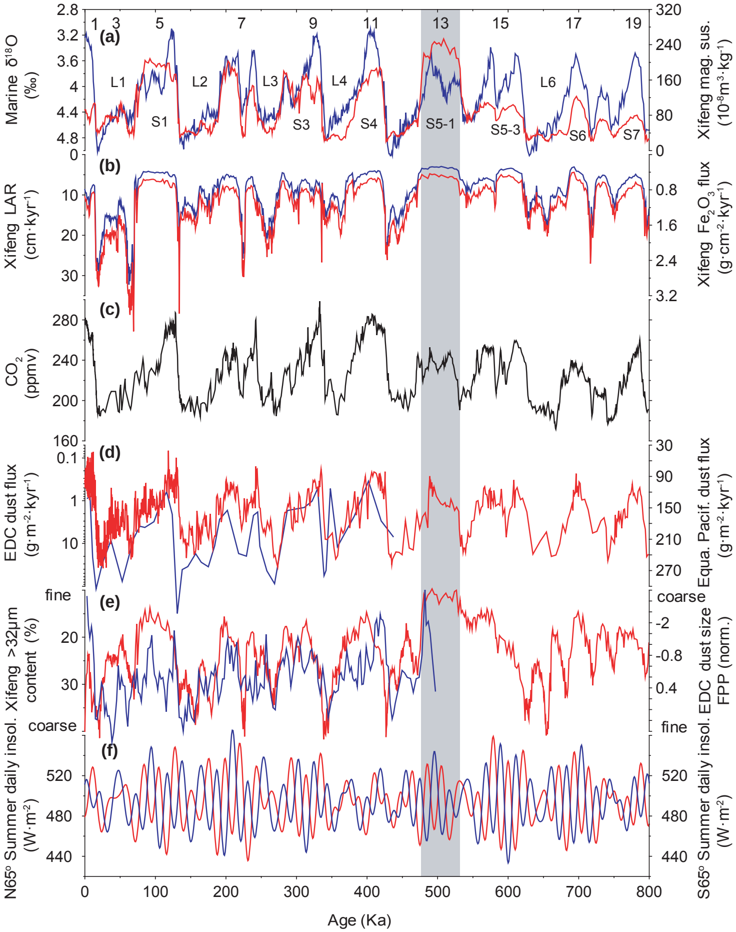

Marine δ18O (‰)
2.8
3.2
3.6
4
4.4
4.8
1
3
5
7
9
11
13
15
17
19
(a)
L1
L2
L3
L4
L6
S1
S3
S4
S5-1
S5-3
S6
S7
320
240
160
80
0
Xifeng mag. sus. (10-8m3·kg-1)
(b)
Xifeng LAR (cm·kyr-1)
0
10
20
30
0.8
1.6
2.4
3.2
Xifeng Fe2O3 flux (g·cm-2·kyr-1)
(c)
CO2 (ppmv)
280
240
200
160
(d)
EDC dust flux (g·m-2·kyr-1)
0.1
1
10
30
90
150
210
270
Equa. Pacif. dust flux (g·m-2·kyr-1)
(e)
fine
coarse
Xifeng >32μm content (%)
20
30
coarse
fine
-2
-0.8
0.4
EDC dust size FPP (norm.)
(f)
N65° Summer daily insol. (W·m-2)
520
480
440
S65° Summer daily insol. (W·m-2)
0
100
200
300
400
500
600
700
800
Age (Ka)

Fig. 2.

Fig. 2. Correlation of the China loess proxies of Asian dust intensity and winter monsoon with relevant ice and marine records. **(a)** Marine δ^{18}O record (Lisiecki and Raymo, 2005) (blue) with the oxygen isotope stages (MIS) labelled at the top part, and loess magnetic susceptibility at Xifeng (red) with the major soil and loess units labelled; **(b)** Loess accumulation rate (LAR, blue) and Fe_2O_3 flux (red) at Xifeng; **(c)** Antarctic (Vostok and EDC) CO_2 records (Luthi et al., 2008;Petit et al., 1999;Siegenthaler et al., 2005); **(d)** EDC (Lambert et al., 2008) (red) and equatorial Pacific (Winckler et al., 2008) (blue) dust fluxes; **(e),** Loess grain-size changes shown by the content of the >32 μm fraction at Xifeng (red) and EDC dust size normalized (Lambert et al., 2008) (blue). **(f)** Summer daily insolation (Berger, 1978) at 65° N (red) and at 65° S (blue). Marine data are plotted versus their own timescales. Antarctic data are plotted versus EDC3 chronology (Parrenin et al., 2007).

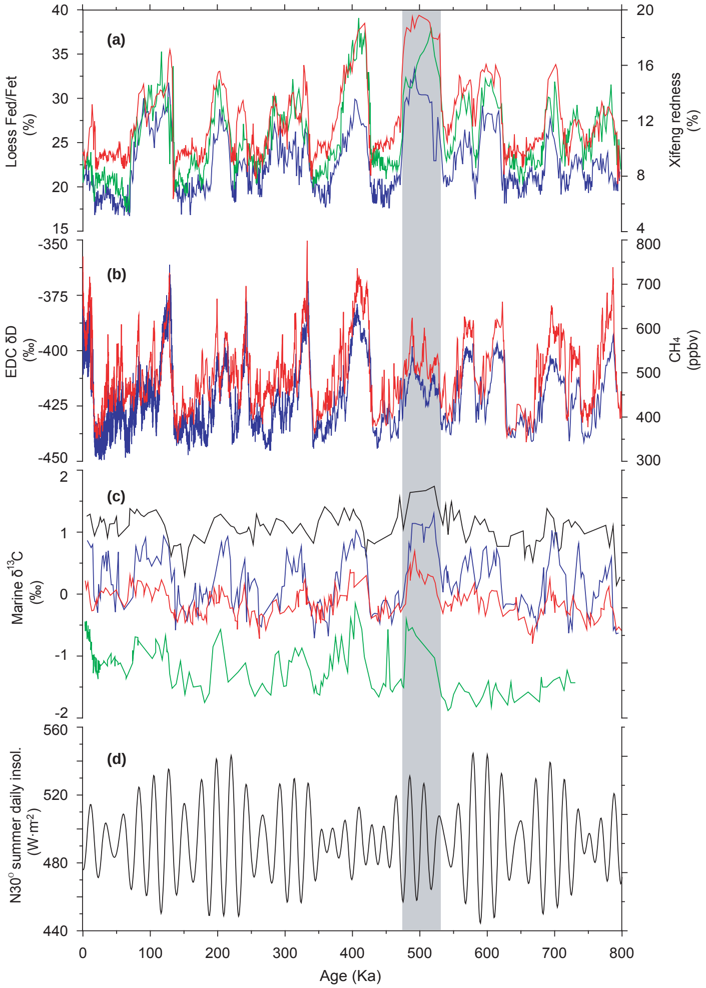
(a)
Loess Fed/Fet (%)
40
35
30
25
20
15
Xifeng redness (%)
20
16
12
8
4
(b)
EDC δD (‰)
-350
-375
-400
-425
-450
CH₄ (ppbv)
800
700
600
500
400
300
(c)
Marine δ13C (‰)
2
1
0
-1
-2
(d)
N30° summer daily insol. (W·m-2)
560
520
480
440
0
100
200
300
400
500
600
700
800
Age (Ka)

Fig. 3.

Fig. 3. Correlation of the China loess proxies of Asian summer monsoon with relevant ice and marine records. **(a)** Chemical weathering index (Guo et al., 2000) (Fed/Fet) at Xifeng (blue), Changwu (green) and the redness at Xifeng (red); **(b)** EDC δD (blue) (Jouzel et al., 2007) and CH_4 record (red) (Loulergue et al., 2008); **(c)** Benthic δ^{13}C records from the North Atlantic site 552 (black) (Raymo et al., 1997), tropical Atlantic site 664 (blue) (Raymo et al., 1997), North Pacific site 849 (red) (Raymo et al., 1997) and Southern Ocean site RC 13-229 (green) (Oppo et al., 1990) versus their own timescales. **(d)** Summer daily insolation (Berger, 1978) at 30° N.